

Force Field Parameters for Large-Scale Computational Modeling of Sensitized TiO₂ Surfaces

Sabas G. Abuabara[†], Jose A. Gascon[†], Cheryl Suet-Yee Leung[†],
Luis G.C. Rego[‡] and Victor S. Batista^{†*}

[†]Department of Chemistry, Yale University, P.O.Box 208107, New Haven, Connecticut 06520-8107, U.S.A.

[‡]Department of Physics, Universidade Federal de Santa Catarina, Florianopolis, SC 88040-900, Brazil

Abstract

Force field parameters for large scale computational modeling of sensitized TiO₂-anatase surfaces are developed from *ab initio* molecular dynamics simulations and geometry optimization based on Density Functional Theory (DFT). The resulting force field, composed of Coulomb, van der Waals and harmonic interactions, reproduces the *ab initio* structures and the phonon spectra density profiles of TiO₂-anatase nanostructures functionalized with catechol, a prototype of an aromatic linker commonly used to sensitize TiO₂ nanoparticles with Ru(II)-polypyridyl dyes. In addition, simulations of interfacial electron injection and electron-hole relaxation dynamics demonstrate the capabilities of the resulting molecular mechanics force-field, as applied in conjunction with mixed quantum-classical methods, for modeling quantum processes that are critical for the overall efficiency of sensitized-TiO₂ solar cells.

Keywords: Semiconductors, solar cells, TiO₂.

I Introduction

The large-scale use of photovoltaic devices for electricity generation is still prohibitively expensive. Fifteen years ago, a promising development emerged with the realization of solar cells based on dye-sensitized TiO₂ films.¹ These photovoltaic devices rapidly achieved light-to-electric energy conversion efficiency as high as 10 % for simulated solar light, exploiting the high surface area of the nanoporous TiO₂ films deposited on conducting glasses. However, attempts to achieve further improvements in efficiency have been hindered by the lack of fundamental understanding of the molecular and electronic processes associated with the constituent operational steps. This problem continues to be a standing challenge, despite significant research effort reported in recent years, including experimental,^{2–18} computational^{19–36} and theoretical^{37–44} studies. It is therefore essential to develop new experiments and theoretical studies to construct realistic models of dye-sensitized TiO₂ interfaces and gain insight on the design of surface-sensitization with optimum photon-to-current conversion efficiency. This paper reports the development of force-field parameters for atomistic modeling of dye-sensitized TiO₂ surfaces and the application of the resulting force field, in conjunction with mixed quantum-classical methods, for simulations of electron-hole pair relaxation dynamics after photoexcitation of TiO₂-anatase sensitized with catechol.

Catechol/TiO₂-anatase nanoparticles are particularly suited for developing and testing force-field parameters for large-scale computations of dye-sensitized TiO₂ surfaces. Catechol has raised significant experimental interest as a prototype of an aromatic linker upon which a wide range of molecular structures can be attached for specific functionalities, including applications to photovoltaic devices with high photon-to-current conversion efficiencies.^{45–47} As a model sensitizer, catechol lowers the TiO₂ absorption threshold

*To whom correspondence should be addressed. Email: victor.batista@yale.edu

from 370 nm to 600 nm, with a shoulder peaking around 420 nm due to a direct charge-transfer excitation from the catechol-HOMO to the conduction band.^{18,20,23,35,36,48–50} In addition, both the structure of the reconstructed catechol/TiO₂ surface and the underlying dynamical processes after photoexcitation of catechol/TiO₂ surface complexes have been characterized at the *ab initio* level.^{30–34} While these previous quantum mechanical studies have provided valuable insight into the nature of dry sensitized TiO₂, studies addressing the role of the solvent and electrolyte environment on recombination redox processes, or the synergistic effects between multiple adsorbates, require large scale simulations beyond the limitations of purely *ab initio* methods.

Simulations of complex molecular environments (*e.g.*, atomistic models with hundreds, or thousands, of atoms) must rely upon molecular mechanics force-fields.^{51–53} Most of these popular force fields are already parametrized to model a wide range of interactions between molecular adsorbates and solvents, or electrolyte species. However, parameters for the interactions with the semiconductor surfaces, or interactions between semiconductors and molecular adsorbates, are still under development. In fact, no force field has so far been widely implemented for modeling functionalized semiconductors, and applications have been limited to those from the development groups, including the description of TiO₂ polymorphs,^{54,55} variable charge schemes for bulk TiO₂,^{56–58} H₂O/TiO₂-rutile interactions,^{59,60} and the adsorption of small organic molecules on TiO₂-rutile.^{61,62} Here, the development of a force-field, composed of Coulomb, van der Waals and harmonic interactions is reported. It is shown that the force-field reproduces the *ab initio* optimized structures and the phonon spectra density profiles of TiO₂-anatase nanostructures functionalized with catechol linkers. In addition, the resulting force field, applied in conjunction with mixed quantum-classical methods, properly describes quantum processes that are critical for the overall efficiency of sensitized-TiO₂ solar cells, including interfacial electron injection and electron-hole relaxation dynamics.

The complexity of the interactions in realistic models of dye-sensitized TiO₂ films, including interactions between the TiO₂ host-substrate and the linkers, adsorbates, solvent molecules and dissolved ions, requires that each component of the system be modeled accurately before attempting to model their interdependent behavior. Considering that significant effort has already been developed on the interactions between molecules and solvents and electrolyte species, the current study focuses only on the interactions in the TiO₂ crystal and the interactions TiO₂-adsorbate. It is therefore natural to expect that the combination of the resulting force field and readily available parameters for adsorbate molecules, solvents and electrolyte species will allow one to investigate a wide range of dyes and (bio)molecular structures which could be attached to TiO₂ surfaces by using aromatic linkers. In particular, the force field is intended for studies that are critical for the design of surface sensitization to optimize charge transport, minimizing recombination and charge trapping mechanisms, including the effect of hydration and redox electrolyte species as well as synergistic effects of multiple adsorbates.

The paper is organized as follows. Section II.1 describes the preparation of structural models and the methodology implemented for *ab initio* molecular dynamics simulations. Section II.2 outlines the methodology implemented for quantum dynamics simulations. Section III.1 describes the development of the force-field in terms of the comparison with structures and energies obtained at the *ab initio*-DFT level. Section III.2 compares the calculations of phonon spectral density profiles obtained from molecular dynamics simulations based on the molecular mechanics force field introduced in this paper and the corresponding benchmark calculations obtained at the *ab initio*-DFT level. Section III.3 tests the resulting force field as applied in conjunction with mixed quantum-classical methods for modeling interfacial electron injection and electron-hole relaxation dynamics. Finally, Sec. IV summarizes and concludes.

II Methods

This section briefly describes the construction of structural models of functionalized TiO₂ nanostructures and the mixed quantum-classical methodology implemented for simulations of electron-hole pair relaxation after photoexcitation of the system. A more thorough description, including details concerning the *ab initio* Molecular Dynamics (MD) simulations and the analysis of structural and electronic properties of the models can be found in previous work.^{30–34}

II.1 Structural Models

The unit cell model system is composed of 32 [TiO₂] units arranged according to the anatase crystalline structure,⁶³ where the (101) surface of the crystal is functionalized with catechol (see Fig. 1). The surface dangling bonds are saturated with hydrogen capping atoms in order to quench the formation of surface states,⁶⁴ avoiding unphysical low coordination numbers. Periodic boundary conditions are imposed with a vacuum spacer between slabs, making negligible the interaction between distinct surfaces in the infinitely periodic model system. Geometry relaxation as well as thermalization and equilibration under conditions of room-temperature and constant volume are performed by using the Vienna *Ab-initio* Simulation Package (VASP/VAMP).^{65,66} The resulting structural relaxation next to the adsorbate describes the underlying surface reconstruction due to functionalization,^{30,67} a process that is partially responsible for quenching the formation of surface states deep within the semiconductor band gap.⁶⁴

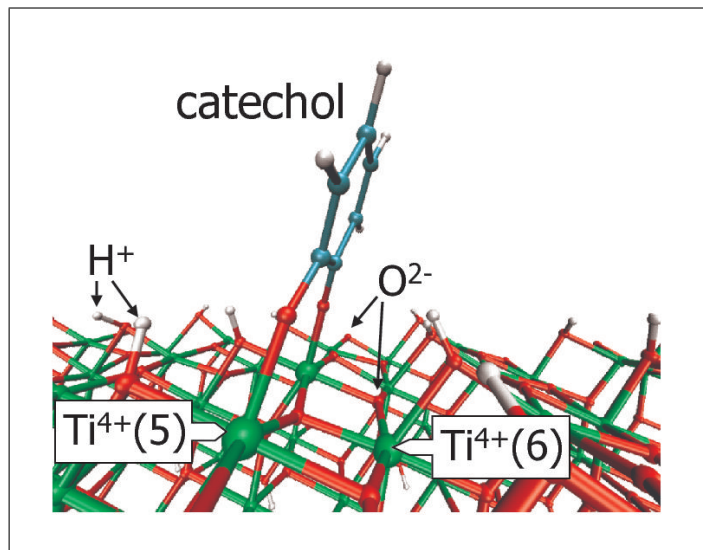


Figure 1: Relaxed configuration of the sensitized TiO₂ nanostructure as described by geometry optimization at the *ab initio*-DFT level. The four types of atoms included in the simulation (Ti,O,C,H) are represented by the colors green, red, turquoise, and white, respectively. The capping hydrogen ions and oxygen ions of the semiconductor lattice are indicated, as is the hexacoordinated Ti⁴⁺ ion near the adsorbate, and the nearest of the two pentacoordinated Ti⁴⁺ ions directly anchoring the catechol adsorbate.

The VASP/VAMP package implements the Density Functional Theory (DFT) in a plane wave basis set, making use of the Perdew-Wang⁶⁸ generalized gradient approximation for the exchange-correlation func-

tional (PW91) and ultrasoft Vanderbilt pseudopotentials for modeling the core electrons.^{69,70} The Kohn-Sham (KS) Hamiltonian is projected onto a plane-wave basis set and high-efficiency iterative methods are used to obtain the KS eigenstates and eigenvalues. Self-consistency is accelerated by means of efficient charge density mixing schemes. Thermal configurations and nuclear trajectories of *ab initio* MD simulations are computed by taking full advantage of the parallelized version of the code with a parallel SP2 supercomputer. The corresponding calculations based on the molecular mechanics force field introduced in this paper are performed by using the program Tinker.⁷¹

II.2 Quantum Dynamics Simulations

Simulations of electronic relaxation, after photoexcitation of adsorbate molecules, are described according to an approximate mixed quantum-classical method, where electrons are treated quantum mechanically and nuclei classically. Nuclear vibrational motion evolves on an effective mean-field Potential Energy Surface (PES), according to classical trajectories $\mathbf{R}^\xi = \mathbf{R}^\xi(t)$ with initial conditions specified by index ξ . Results are obtained by sampling an ensemble of initial conditions ξ for nuclear motion, integrating the Time-Dependent Schrödinger Equation (TDSE), over the corresponding *ab initio*-DFT nuclear trajectories and averaging expectation values over the resulting time-evolved wavefunctions. Converged results for finite temperature simulations are typically obtained by averaging over fewer than 50 initial conditions, representing the system thermalized under conditions of room-temperature and constant volume. However, finite temperature results are reported for averages over 100 initial conditions. The appreciation of conditions under which quantum coherences may be described according to mixed quantum-classical methodologies has been the subject of intense research,^{72–75} including the analysis of decoherence in similar composite models.^{76,77} The applicability of mixed quantum-classical dynamics is found to be valid so long as the quantum subsystem (electronic dynamics) decoheres slowly and the remainder (nuclear dynamics), often coupled to a thermal bath, decoheres quickly.⁷⁸

Propagation of the time-dependent electronic wave function is performed for each nuclear trajectory $\mathbf{R}^\xi(t)$ by numerically exact integration of the TDSE,

$$\{i\hbar\partial/\partial t - \mathbf{H}(t)\}|\Psi^\xi(t)\rangle = 0. \quad (1)$$

Here, $\mathbf{H}(t)$ is described according to a tight binding model Hamiltonian gained from the extended Hückel (EH) approach.^{79,80} The EH Hamiltonian is computed in the basis of Slater-type orbitals χ for the radial part of the atomic orbital (AO) wavefunctions,^{30,81} including the 4s, 4p and 3d atomic orbitals of Ti^{4+} ions, the 2s and 2p atomic orbitals of O^{2-} ions, the 2s and 2p atomic orbitals of C atoms, and the 1s atomic orbitals of H atoms. The AOs $\{|\chi_\alpha(t)\rangle\}$ form a mobile (nonorthogonal) basis set due to nuclear motion, with $S_{\alpha\beta}(t) = \langle\chi_\alpha(t)|\chi_\beta(t)\rangle$ the corresponding time-dependent overlap matrix elements. The overlap matrix is computed using periodic boundary conditions along the [010] or [-101] directions, for the [-101] and [010] extended systems, respectively. Advantages of this method, relative to plane-wave approaches, are that it requires a relatively small number of transferable parameters and is capable of providing accurate results for the energy bands of elemental materials (including transition metals) as well as compound bulk materials in various phases.⁸⁰ In addition, the EH method is applicable to large extended systems and provides valuable insight on the role of chemical bonding.⁸²

The time-dependent hole wavefunction,

$$|\Psi^\xi(t)\rangle = \sum_q B_q(t)|\phi_q(t)\rangle, \quad (2)$$

is expanded in the basis of instantaneous eigenstates $|\phi_q(t)\rangle = \sum_\alpha C_{\alpha,q}(t)|\chi_\alpha(t)\rangle$ of the generalized eigenvalue problem $\mathbf{H}(t)\mathbf{C}(t) = \mathbf{S}(t)\mathbf{C}(t)\mathbf{E}(t)$, with eigenvalues $E_q(t)$. It is assumed that the initial state consists

of an electronic excitation localized in the lowest unoccupied molecular orbital (LUMO) of the central (C) surface complex.

The propagation scheme is based on the recursive application of the short-time approximation

$$|\Psi^\xi(t + \tau/2)\rangle \approx \sum_q B_q(t) e^{-\frac{i}{\hbar} E_q(t)\tau/2} |\phi_q(t)\rangle. \quad (3)$$

The evolution of the expansion coefficients

$$B_q(t + \tau) = \sum_p B_p(t) e^{-\frac{i}{\hbar} [E_p(t) + E_q(t+\tau)]\tau/2} \langle \phi_q(t + \tau) | \phi_p(t) \rangle \quad (4)$$

is approximated by

$$B_q(t + \tau) \approx B_q(t) e^{-\frac{i}{\hbar} [E_q(t) + E_q(t+\tau)]\tau/2}, \quad (5)$$

in the limit of sufficiently thin time-slices τ .

The relaxation dynamics is quantitatively described in terms of expectation values of observables computed as $\langle \hat{A} \rangle = \text{Tr}\{\hat{\rho}(t)\hat{A}\}$, where $\hat{\rho}(t)$ is the reduced density operator associated with the electronic degrees of freedom,

$$\hat{\rho}(t) = \sum_\xi p_\xi |\Psi^\xi(t)\rangle \langle \Psi^\xi(t)|, \quad (6)$$

with p_ξ the probability of sampling initial conditions, specified by index ξ , associated with the thermal ensemble of nuclear configurations.

The time-dependent electronic populations are determined as follows:

$$\mathbf{P}_j(t) = \text{Tr}\{\hat{\rho}(t)\hat{P}_j\}, \quad (7)$$

where \hat{P}_j is the projection operator onto the subset of atomic orbitals of interest. Computations of the transient electron(hole) populations $\mathbf{P}_j(t)$ of the molecular adsorbate j are defined accordingly,

$$\hat{P}_j = \sum_{\alpha, \beta \in j} |\chi_\alpha\rangle (S^{-1})_{\alpha\beta} \langle \chi_\beta|, \quad (8)$$

where the sum over atomic orbitals includes atoms of adsorbate j only.

III Results

III.1 Force Field Parameters

The force field parameters (see supporting information) were adopted as much as possible from the force fields Amber94⁵¹ and OPLS-AA.⁵² The electrostatic and Van der Waals interactions are described by the sum of Coulomb and Lennard-Jones potentials,

$$V = \sum_i \sum_j \left[q_i q_j e^2 / r_{ij} + 4\epsilon_{ij} \left(\frac{\sigma_{ij}}{r_{ij}} \right)^{12} - 4\epsilon_{ij} \left(\frac{\sigma_{ij}}{r_{ij}} \right)^6 \right] f_{ij}, \quad (9)$$

between all pairs of atoms i and j with ($i < j$) separated by three or more bonds. Here, $f_{ij} = 1.0$, except for intramolecular 1,4-interactions for which $f_{ij} = 0.5$. However, Van der Waals interactions are neglected for the host-substrate since they represent only minor contributions to the energy of the TiO_2 crystal.

The TiO_2 ionic charges are obtained from the electronic population analysis of the sensitized nanostructure unit cell as described by the *ab initio*-DFT level of theory. Stretching and bending energies are described by harmonic potentials with equilibrium bond-lengths r_{eq} and equilibrium angles θ_{eq} that are fitted to reproduce the relaxed configuration of the unit cell obtained by geometry optimization at the DFT-*ab initio* level. Harmonic constants K_r and K_θ were fitted to reproduce the *ab initio* phonon spectral density. Initial guess parameters for TiO_2 were based on the Morse-stretch potentials of MS-Q models,⁵⁸ while the constants for the adsorbate molecule were taken from the force fields OPLS-AA⁵² and Amber94.⁵¹

The comparison between optimized configurations of sensitized TiO_2 nanostructures, obtained at the *ab initio*-DFT level and according to the molecular mechanics force field indicate that both calculations predict essentially the same optimized structures. In fact, the resulting root-mean-squared (rms) between the two relaxed configurations is $\text{rms} = 0.3 \text{ \AA}$. Relaxed structures were obtained by optimizing the energy of the system with respect to the geometry of the anchored catechol molecule and the 6 top-most layers in the semiconductor surface, including the capping hydrogen atoms in the upper layer. Relative to the bulk TiO_2 structure, there are significant rearrangements associated with the Ti^{4+} and O^{2-} ions next to the molecular adsorbate. Further, the alignment of the catechol adsorbate along the [100] direction is determined by the electronic repulsion with the nearby row of di-coordinated O^{2-} ions. Such electrostatic repulsion is also responsible for displacing the two-fold coordinated O^{2-} ions and for stretching their bonds with the hexa-coordinated Ti^{4+} ions next to the molecular adsorbate. Far from the attachment site, however, the geometry of the anatase crystal is in agreement with previous theoretical calculations of TiO_2 -anatase.⁶³

III.2 Phonon Spectral Density

Figure 2 shows the comparison of the total phonon spectral density and the individual components associated with the adsorbate and the host-substrate, obtained from molecular dynamics simulations of the catechol/ TiO_2 -anatase model system described in Sec. II.1. The phonon spectral density has been computed as the Fourier transform of the velocity autocorrelation function obtained from molecular dynamics simulations at 300 K and constant volume. Results obtained according to *ab initio*-DFT molecular dynamics are compared to the corresponding results based on the classical mechanics force-field. Figure 2 shows that the force field predicts the vibrational frequencies for both the adsorbate molecules and the TiO_2 -anatase semiconductor, as well as the relative intensities in the phonon spectra density profile, in very good agreement with *ab initio* calculations. The vibrational frequencies are also in good agreement with the experimental normal mode frequencies.^{83,84}

As discussed in Ref. [30], the more prominent peaks in the total spectral density correspond to the O-H stretching motion of H capping atoms on the TiO_2 -anatase surface and the C-H stretching motion in the catechol molecule, at 3700 cm^{-1} and 3100 cm^{-1} , respectively. The normal modes of TiO_2 -anatase are in the $262\text{--}876 \text{ cm}^{-1}$ range, in agreement with experimental measurements.⁸⁴ These vibrational periods are expected to be only marginally affected by photoexcitation of the adsorbate molecule, or the injection of an electron to the conduction band. Especially, considering that the TiO_2 frequencies correspond to the characteristic vibrational period of 40 fs, which is an order of magnitude larger than the ultrafast time scale associated with the primary electron injection event.³⁰⁻³⁴ In addition, the vibrational frequencies of the catechol molecule are only slightly affected by photo-excitation of the molecule to the S_1 electronic state.⁸⁴

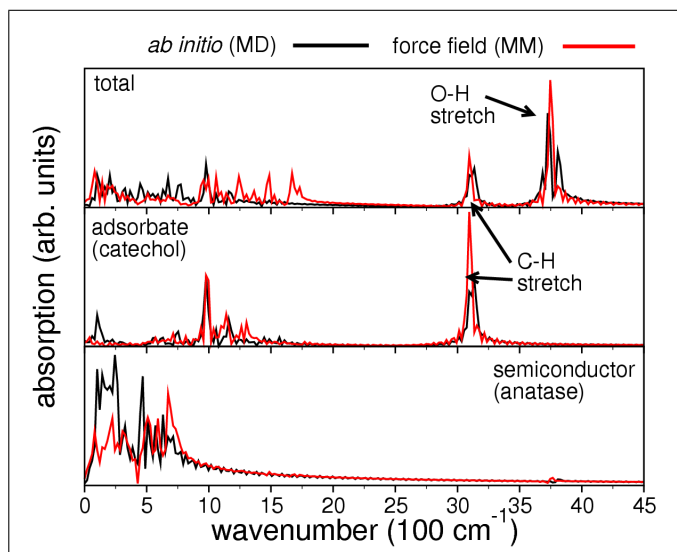


Figure 2: Comparison of total phonon spectral density (upper panel) of the catechol/TiO₂-anatase model system, introduced in Sec. II.1, and individual contributions due to nuclear motion in the adsorbates (middle panel) and the TiO₂-anatase host substrate, as described by molecular dynamics simulations based on *ab initio*-DFT (black) and the molecular mechanics force field introduced in this paper (red).

III.3 Electron-Injection Dynamics

Figure 3 shows the evolution of the time-dependent adsorbate population, after instantaneously populating the catechol-LUMO. These results are obtained according to the mixed quantum-classical methodology, described in Sec. II.2, in conjunction with molecular dynamics simulations based on either *ab initio*-DFT, or the molecular mechanics force field introduced in Sec. III.1.

Figure 3 shows that both levels of theory predict that the overall relaxation dynamics at room temperature is largely described by a single exponential decay with a characteristic time $\tau \simeq 2.5$ fs, reaching complete transfer within 10 fs. The initial electronic state is chosen to correspond closely to the native catechol-LUMO of the photo-excited surface-complex, a state that is a critical component of the electronic states of dyes with high photo-to-current conversion efficiencies (*e.g.*, catechol para-substituted with Ru(II)-polypyridyl complexes). As pointed out by Grätzel, Nozik, Lian, and others,^{2,3,17,46,85} efficient photo-injection mechanisms from larger organometallic dye molecules involve reaction pathways via these higher electronic states of the aromatic linker (*i.e.*, Metal-to-Ligand Charge Transfer states (MLCTs) involving the π^* levels). The reported results are also relevant to the electron injection dynamics from the native excited states of catechol, even in the presence of competing direct catechol-TiO₂ charge-transfer excitations. ‘Vertical’ transitions to higher-energy electronic states localized in the surface complexes (*e.g.*, corresponding more closely to the catechol HOMO-LUMO and HOMO-(LUMO+1) states) are quantum mechanically allowed^{20,23,50} due to the rigidity of the catechol-anatase system limiting the direct coupling between the adsorbate π system and the semiconductor substrate.

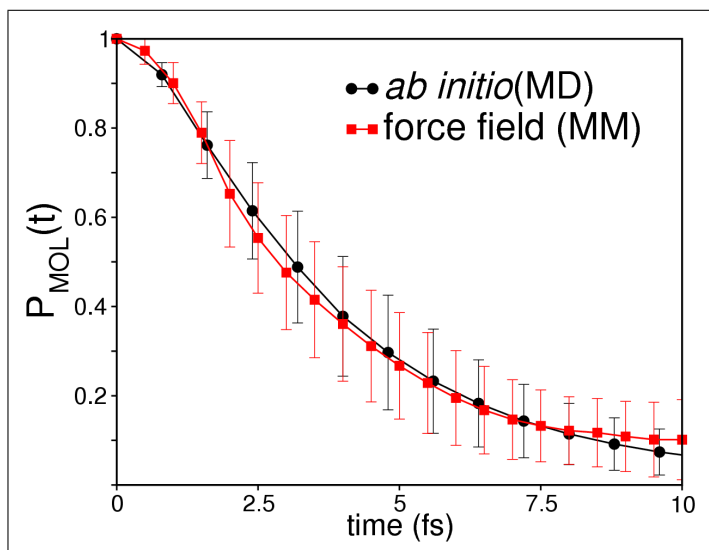


Figure 3: Comparison of the time dependent adsorbate population, after instantaneously populating the catechol-LUMO, in sensitized nanostructures extended along the [-101] crystallographic direction of the anatase crystal. Mixed quantum-classical calculations based on the molecular mechanics force field introduced in this paper (red squares) are compared to the corresponding results based on *ab initio*-DFT molecular dynamics.

IV Concluding Remarks

We have described the development and testing of force field parameters for large-scale computational modeling of sensitized TiO_2 surfaces. Stretching and bending equilibrium parameters were derived to reproduce the relaxed configuration of the catechol/ TiO_2 unit cell nanostructure, obtained by geometry optimization at the DFT-*ab initio* level. Harmonic force constants for stretching and bending motion were fitted to reproduce the *ab initio* phonon spectral density of the unit cell nanostructure. The quality of the resulting force field was evaluated as applied in conjunction with mixed quantum-classical methods for the description of the electron-hole relaxation dynamics after excitation of molecular adsorbates.

Testing the resulting force field for predictions of *ab initio* optimized structures, phonon spectral density profiles, and the influence of thermal nuclear fluctuations on the electron relaxation dynamics after excitation of surface complexes has been the main topic of the paper. The validation is crucial since the force field parameters are intended for applications beyond the capabilities of purely *ab initio* methods. Such large-scale atomistic simulations will allow one to address processes that are critical for the overall efficiency of sensitized- TiO_2 solar cells, including the synergistic effects between multiple adsorbates as well as the influence of the solvent and the electrolyte environment on the dynamics of electron injection and recombination.

V Acknowledgment

V.S.B. acknowledges supercomputer time from the National Energy Research Scientific Computing (NERSC) Center and financial support from Research Corporation, Research Innovation Award # RI0702, a Petroleum Research Fund Award from the American Chemical Society PRF # 37789-G6, a junior faculty

award from the F. Warren Hellman Family, the National Science Foundation (NSF) Career Program Award CHE # 0345984, the NSF Nanoscale Exploratory Research (NER) Award ECS # 0404191, the Alfred P. Sloan Fellowship (2005-2006) from the Sloan Foundation, a Camille Dreyfus Teacher-Scholar Award for 2005, a Yale Junior Faculty Fellowship in the Natural Sciences (2005), and start-up package funds from the Provost's office at Yale University.

References

- [1] B. O'Regan and M. Grätzel. *Nature*, 353:737–739, 1991.
- [2] J. B. Asbury, R. J. Ellingson, H. N. Ghosh, S. Ferrere, A. J. Nozik, and T. Q. Lian. *J. Phys. Chem. B*, 103:3110–3119, 1999.
- [3] J. B. Asbury, E. Hao, Y. Q. Wang, H. N. Ghosh, and T. Q. Lian. *J. Phys. Chem. B*, 105:4545–4557, 2001.
- [4] J. B. Asbury, N. A. Anderson, E. Hao, X. Ai, and T. Q. Lian. *J. Phys. Chem. B*, 107:7376–7386, 2003.
- [5] N. A. Anderson, X. Ai, and T. Q. Lian. *J. Phys. Chem. B*, 107:14414–1421, 2003.
- [6] C. Bauer, G. Boschloo, E. Mukhtar, and Hagfeldt A. *Int. J. Photoenergy*, 4:17–20, 2002.
- [7] R. Huber, J. E. Moser, M. Grätzel, and J. Wachtveitl. *J. Phys. Chem. B.*, 106:6494–6499, 2002.
- [8] J. Schnadt, P. A. Brühwiler, L. Patthey, J. N. O'Shea, S. Sodergren, M. Odelius, R. Ahuja, O. Karis, M. Bassler, and P. Persson. *Nature*, 418:620–623, 2002.
- [9] J. Schnadt, J. N. O'Shea, L. Patthey, L. Kjeldgaard, J. Ahlund, K. Nilson, J. Schiessling, J. Krem-pasky, M. Shi, O. Karis, C. Glover, H. Siegbahn, N. Martensson, and P. A. Bruhwiler. *J. Chem. Phys.*, 119:12462–12472, 2003.
- [10] J. Schnadt, A. Henningsson, M. P. Andersson, P. G. Karlsson, P. Uvdal, H. Siegbahn, P. A. Brühwiler, and A. Sandell. *J. Phys. Chem. B*, 108:3114–3122, 2004.
- [11] F. Willig, C. Zimmerman, S. Ramakrishna, and W. Storck. *Electrochem. Acta*, 45:4565–4575, 2000.
- [12] C. Zimmerman, F. Willig, S. Ramakrishna, B. Burfeindt, B. Pettinger, R. Eichberger, and W. Storck. *J. Phys. Chem. B.*, 105:9245–9253, 2001.
- [13] L. Gundlach, R. Ernstorfer, and F. Willig. *Phys. Rev. B*, 74:035324, 2006.
- [14] T. Hannappel, B. Burfeindt, W. Storck, and F. Willig. *J. Phys. Chem. B.*, 101:6799–6802, 1997.
- [15] G. Ramakrishna, A. K. Singh, D. K. Palit, and H. N. Ghosh. *J. Phys. Chem B*, 108:1701–1707, 2004.
- [16] G. Ramakrishna, A. K. Singh, D. K. Palit, and H. N. Ghosh. *J. Phys. Chem B*, 108:4775–4783, 2004.
- [17] G. Ramakrishna, A. K. Singh, D. K. Palit, and H. N. Ghosh. *J. Phys. Chem B*, 108:12489–12496, 2004.
- [18] J. Moser, S. PUNCHIHEWA, P. P. Infelta, and M. Grätzel. *Langmuir*, 7:3012–3018, 1991.
- [19] P. Persson, S. Lunell, and L. Ojamae. *Chem. Phys. Lett.*, 364:469–474, 2002.
- [20] P. Persson, R. Bergström, and S. Lunell. *J. Phys. Chem. B*, 104:10348–10351, 2000.

- [21] P. Persson and M. D. Lundqvist. *J. Phys. Chem. B*, 109:11918–11924, 2005.
- [22] W. R. Duncan, W. Stier, and O. V. Prezhdo. *J. Am. Chem. Soc.*, 127:7941–7951, 2005.
- [23] W. R. Duncan and O. V. Prezhdo. *J. Phys. Chem. B*, 109:365–373, 2005.
- [24] B. B. Smith and A. J. Nozik. *J. Phys. Chem. B*, 103:9915–9932, 1999.
- [25] B. B. Smith and A. J. Nozik. *J. Phys. Chem. B*, 205:47–72, 1996.
- [26] W. Stier and O. V. Prezhdo. *J. Mol. Struct-Theochem.*, 630:33–43, 2003.
- [27] W. Stier and O. V. Prezhdo. *J. Phys. Chem B*, 106:8047–8054, 2002.
- [28] W. Stier, W. R. Duncan, and O. V. Prezhdo. *Adv. Mater.*, 16:240–244, 2004.
- [29] Thoss M., Kondov I., and Wang H. B. *Chem. Phys.*, 304:169–181, 2004.
- [30] L. G. C. Rego and V. S. Batista. *J. Am. Chem. Soc.*, 125:7989–7997, 2003.
- [31] L. G. C Rego, S. G. Abuabara, and V. S. Batista. *J. Chem. Phys.*, 122:154709, 2005.
- [32] L. G. C Rego, S. G. Abuabara, and V. S. Batista. *Quantum. Inform. Compu.*, 5:318–334, 2005.
- [33] L. G. C Rego, S. G. Abuabara, and V. S. Batista. *J. Mod. Optics*, 2006. in press.
- [34] L. G. C. Rego and V. S. Batista. *J. Am. Chem. Soc.*, 127:18234–18242, 2005.
- [35] P. C. Redfern, P. Zapol, L. A. Curtiss, T. Rajh, and M. C. Thurnauer. *J. Phys. Chem. B*, 107:11419–11427, 2003.
- [36] F. De Angelis, A. Tilocca, and A. Selloni. *J. Am. Chem. Soc.*, 126:15024–15025, 2004.
- [37] S. Ramakrishna and F. Willig. *J. Phys. Chem. B.*, 104:68–77, 2000.
- [38] S. Ramakrishna, F. Willig, and V. May. *J. Chem. Phys.*, 115:2743–2756, 2001.
- [39] Y. G. Boroda and G. A. Voth. *J. Chem. Phys.*, 104:6168–6183, 1996.
- [40] Y. G. Boroda, A. Calhoun, and G. A. Voth. *J. Chem. Phys.*, 107:8940–8954, 1997.
- [41] A. A. Kornyshev and W. Schmickler. *J. Electroanal. Chem.*, 185:253–261, 1985.
- [42] A. Petersson, M. A. Ratner, and H. O. Karlsson. *J. Phys. Chem. B*, 104:8498–8502, 2000.
- [43] Y. Q. Gao, Y. Georgievskii, and R. A. Marcus. *J. Chem. Phys.*, 112:3358–3369, 2000.
- [44] Y. Q. Gao and R. A. Marcus. *J. Chem. Phys.*, 113:6351–6360, 2000.
- [45] C. R. Rice, M. D. Ward, M. K. Nazeeruddin, and M. Grätzel. *New J. Chem.*, 24:651–652, 2000.
- [46] R. Mosurkal, J. A. He, K. Yang, L. A. Samuelson, and J. Kumar. *J. Photochem. Photobio. A.*, 168:191–196, 2004.
- [47] E. Galoppini. *Coord. Chem. Rev.*, 248:1283–1297, 2004.
- [48] R. Rodriguez, M. A. Blesa, and A. E. Regazzoni. *J. Colloid. Interf. Sci.*, 177:122–131, 1996.

- [49] Y. Liu, J. I. Dadap, D. Zimdars, and K. B. Eisenthal. *J. Phys. Chem. B*, 103:2480–2486, 1999.
- [50] Y. H. Wang, K. Hang, N. A. Anderson, and T. Q. Lian. *J. Phys. Chem. B*, 107:9434–9440, 2003.
- [51] W. D. Cornell, P. Cieplak, C. I. Bayly, I. R. Gould, K. M. Merz, D. M. Ferguson, D. C. Spellmeyer, T. Fox, J. W. Caldwell, and P. A. Kollman. *J. Am. Chem. Soc.*, 117:5179–5197, 1995.
- [52] W. L. Jorgensen, D. S. Maxwell, and J. Tirado Rives. *J. Am. Chem. Soc.*, 118:11225–11236, 1996.
- [53] A. D. MacKerell, A. Bashford, M. Bellott, R. L. Dunbrack, J. D. Evanseck, M. J. Field, S. Fischer, J. Gao, H. Guo, S. Ha, D. Joseph-McCarthy, L. Kuchnir, K. Kuczera, F. T. K. Lau, C. Mattos, S. Michnick, T. Ngo, D. T. Nguyen, B. Prodhom, W. E. Reiher, B. Roux, M. Schlenkrich, J. C. Smith, R. Stote, J. Straub, M. Watanabe, J. Wiorkiewicz-Kuczera, D. Yin, and M. Karplus. *J. Phys. Chem. B*, 102:3586–3616, 1998.
- [54] M. Matsui and M. Akaogi. *Mol. Simul.*, 6:239, 1991.
- [55] D. W. Kim, N. Enomoto, and Z. Nakagawa. *J. Am. Ceram. Soc.*, 79:1095–1099, 1996.
- [56] A. K. Rappe and W. A. Goddard III. *J. Phys. Chem.*, 95:3358, 1991.
- [57] V. Swamy and J. D. Gale. *Phys. Rev. B*, 62:5406, 2000.
- [58] B. S. Thomas, N. A. Marks, and B. D. Begg. *Phys. Rev. B*, 69:144122, 2004.
- [59] A. V. Bandura and J. D. Kubicki. *J. Phys. Chem. B*, 107:11072–11081, 2003.
- [60] A. V. Bandura, D. G. Sykes, V. Shapovalov, T. N. Troung, J. D. Kubicki, and R. A. Evarestov. *J. Phys. Chem. B*, 108:7844–7853, 2004.
- [61] S. Suzuki, Y. Yamaguchi, H. Onishi, T. Sasaki, K. Fukui, and Y. Iwasawa. *J. Chem. Soc., Faraday Trans.*, 94:161–166, 1998.
- [62] M. L. Sushko, A. Y. Gal, and A. L. Shluger. *J. Phys. Chem. B*, 110:4853–4862, 1987.
- [63] A. Vittadini, A. Selloni, F. P. Rotzinger, and M. Gratzel. *J. Phys. Chem. B*, 104:1300, 2000.
- [64] W. Mönch. In *Semiconductor Surfaces and Interfaces*. Springer, Berlin, 1993.
- [65] G. Kresse and J. Furthmüller. *Phys. Rev. B*, 54:11169–11186, 1996. <http://cms.mpi.univie.ac.at/vasp/>.
- [66] G. Kresse and J. Furthmüller. *Comp. Mat. Sci.*, 6:15–50, 1996.
- [67] U. Diebold. *Surf. Sci. Rep.*, 48:53–229, 2003.
- [68] J. P. Perdew. In P. Ziesche and H. Eschrig, editors, *Electronic Structure of solids '91*. Akademie Verlag, Berlin, 1991.
- [69] D. Vanderbilt. *Phys. Rev. B*, 41:7892–7895, 1990.
- [70] K. Laasonen, A. Pasquarello, R. Car, C. Lee, and D. Vanderbilt. *Phys. Rev. B*, 47:10142–10153, 1993.
- [71] J. W. Ponder. *Tinker, version 3.9*, 2001. Washington University School of Medicine, St. Louis, Missouri.
- [72] W. H. Zurek. *Phys. Rev. D*, 24:1516, 1981.

- [73] W. H. Zurek. *Phys. Rev. D*, 26:1862, 1981.
- [74] E. Joos and H. D. Zeh. *Z. Phys. B: Condens. Matter*, 59:223, 1985.
- [75] E. Joos, H. D. Zeh, C. Kiefer, D. Giulini, J. Kupsch, and I. O. Stamatescu. In *Decoherence and the Appearance of a Classical World in Quantum Theory*. Springer-Verlag, Berlin Heidelberg, 1996.
- [76] E. R. Bittner and P. J. Rossky. *J. Chem. Phys.*, 103:8130, 1995.
- [77] O. V. Prezhdo and P. J. Rossky. *Phys. Rev. Lett.*, 81:5294, 1998.
- [78] K. Shiokawa and R. Kapral. *J. Chem. Phys.*, 117:7852, 2002.
- [79] S. P. McGlynn, L. G. Vanquickenborne, M. Kinoshita, and D. G. Carroll. Holt, Rinehart, and Winston INC., New York, 1972.
- [80] J. Cerda and F. Soria. *Phys. Rev. B*, 61:7965–7971, 2000.
- [81] For a numerical implementation of the method: Landrum, G. A. and Glassy, W. V. , *The YAEHMOP project*, <http://yaehmop.sourceforge.net>.
- [82] M. R. Hoffmann. *Rev. Mod. Phys.*, 60:601–628, 1988.
- [83] M. Gerhards, W. Perl, S. Schumm, U. Henrichs, C. Jacoby, and K. Kleinermanns. *J. Chem. Phys.*, 104:9362–9375, 1996.
- [84] R. J. Gonzalez, R. Zallen, and H. Berger. *Phys. Rev. B*, 55:7014–7017, 1997.
- [85] A. Hagfeldt and M. Grätzel. 95:49–68, 1995.